Koland, J. G., Miller, M. J., & Gennis, R. B. (1984b) *Biochemistry 23*, 1051-1056.
Kranz, R. G., & Gennis, R. B. (1984) *J. Biol. Chem. 259*, 7998-8003.
Lorence, R. M., & Gennis, R. B. (1989) *J. Biol. Chem. 264*, 7135-7140.
Lorence, R. L., Green, G. N., & Gennis, R. B. (1984) *J. Bacteriol. 157*, 115-121.
Lorence, R. M., Koland, J. G., & Gennis, R. B. (1986) *Biochemistry 25*, 2314-2321.
Lorence, R. M., Carter, K., Gennis, R. G., Matsushita, K., & Kaback, H. R. (1988) *J. Biol. Chem. 263*, 5271-5276.
Matsudaira, P. T. (1987) *J. Biol. Chem. 262*, 10035-10038.
Meinhardt, S. W., Gennis, R. G., & Ohnishi, T. (1989) *Biochim. Biophys. Acta 975*, 175-184.
Miller, M. J., & Gennis, R. B. (1983) *J. Biol. Chem. 258*, 9159-9165.
Miller, M. J., & Gennis, R. B. (1985) *J. Biol. Chem. 260*, 14003-14008.
Miller, M. J., Hermodson, M., & Gennis, R. B. (1988) *J. Biol. Chem. 263*, 5235-5240.
Minghetti, K. C., & Gennis, R. B. (1988) *Biochem. Biophys. Res. Comm. 155*, 243-248.
Rice, C. W., & Hempfling, W. P. (1978) *J. Bacteriol. 134*, 115-124.
Smith, A., Hill, S., & Anthony, C. (1990) *J. Gen. Microbiol. 136*, 171-180.
Yang, F. D., Yu, L., Yu, C. A., Lorence, R. M., & Gennis, R. B. (1986) *J. Biol. Chem. 261*, 14987-14990.

Time-Resolved Fluorescence Studies of Genetically Engineered *Escherichia coli* Glutamine Synthetase. Effects of ATP on the Tryptophan-57 Loop†

William M. Atkins,‡ Patrick S. Stayton,§ and Joseph J. Villafranca*,‡

Department of Chemistry, The Pennsylvania State University, University Park, Pennsylvania 16802, and Department of Biochemistry, University of Illinois, Urbana, Illinois 61801

Received August 1, 1990; Revised Manuscript Received January 7, 1991

ABSTRACT: Single-tryptophan-containing mutants of low adenylylation state *Escherichia coli* glutamine synthetase (wild type has two tryptophans at positions 57 and 158) have been constructed and studied by multifrequency phase/modulation fluorescence spectroscopy. The W57L mutant (retains tryptophan at residue 158) and the W158S mutant (retains tryptophan at residue 57) are both characterized by heterogeneous exponential decay kinetics. Global analysis indicates that for the Mn-bound form of the enzyme at pH 7.4 the fluorescence of both tryptophans is best described by a sum of three discrete exponentials with recovered lifetimes of 4.77, 1.72, and 0.10 ns for Trp-57 and 5.04, 2.28, and 0.13 ns for Trp-158. The wild-type enzyme also exhibits decay kinetics described by a triple-exponential model with similar lifetime components. The individual tryptophans are distinguishable by the fractional intensities of the resolvable lifetimes. The wild-type and W158S enzymes are dominated by the 5-ns component which provides nearly 60% and 65%, respectively, of the fractional intensity at five wavelengths spanning the emission spectrum. In contrast, the W57L enzyme demonstrates a larger fraction of the 2-ns lifetime species (60%) and only 35% of the longer lifetime component. The substrate ATP induces a shift to approximately 90% of the 5-ns component for the wild-type and W158S enzymes, whereas the W57L protein is essentially unaffected by this ligand. Steady-state quenching studies with iodide indicate that addition of ATP results in a 3.0-3.5-fold decrease in the apparent Stern-Volmer quenching constants for the wild-type and W158S enzymes. Phase/modulation experiments at several iodide concentrations indicate that the median, 2 ns, lifetime component is selectively quenched compared to the 5-ns lifetime component. These results suggest a model where ATP binding results in a shift in the equilibrium distribution of microconformational states populated by Trp-57. ATP shifts this equilibrium nearly completely to the states exhibiting the long-lifetime component which, based on quenching studies, is less solvent-accessible than the conformational states associated with the other lifetime components.

The dynamic nature of proteins, an essential aspect of their function, is exemplified by rotational motions of amino acid side chains, microconformational heterogeneity of localized peptide segments, and ligand-induced changes in domain structure and conformation (Demchenko, 1986; DeBrunner & Fraunfelder, 1982). These types of molecular motion are amenable to study by various types of fluorescence spectroscopies which sensitively reflect changes in the local environment of many fluorophores, including changes which take place on the nanosecond time scale (Alcala et al., 1987; Demchenko, 1986; Lakowicz, 1983). We have utilized phase/modulation and steady-state fluorescence techniques with site-directed mutants to determine the nature of the local environment of the individual tryptophan residues of *Escherichia coli* glut-

† This research was supported by NIH Grants GM-23529 (J.J.V) and GM-13714 (W.M.A.) and by a grant to the Laboratory for Fluorescence Dynamics (LFD) at the University of Illinois through the Division of Research Resources of the NIH (RR031555 01) and the University of Illinois at Urbana—Champaign.
* To whom correspondence should be addressed.
‡ The Pennsylvania State University.
§ University of Illinois.

0006-2960/91/0430-3406$02.50/0

amine synthetase (Trp-57 and Trp-158).

Glutamine synthetase (GS)[1] catalyzes the ATP-dependent condensation of glutamate with ammonia to afford glutamine, ADP, and P_i (Stadtman & Ginsburg, 1974; Ginsburg, 1972). The enzyme from *E. coli* is a dodecamer of identical subunits (MW 51 814) arranged as two face-to-face hexagonal rings (Valentine et al., 1968; Frey et al., 1975). Catalysis requires two metal ions per subunit (Mn^{2+} or Mg^{2+}) and proceeds by a stepwise mechanism involving the formation of γ-glutamyl phosphate followed by nucleophilic attack by enzyme-bound NH_3 on the γ-carbonyl group. Studies on the kinetic mechanism suggest a preferred ordered scheme with ATP binding followed by glutamate and NH_4^+ (Meek & Villafranca, 1980; Colanduoni et al., 1982). The high-resolution X-ray crystal structure of the Mn-bound form of the *Salmonella typhimurium* enzyme, which differs from the *E. coli* structure by only 10 amino acids, has provided an extremely valuable model for understanding the structure–function relationships of this enzyme (Almassy et al., 1986; Yamashita et al., 1989), but does not provide information concerning various liganded states of the protein and their relative dynamic nature. The recent cloning and characterization of the gene encoding *E. coli* GS (Colombo & Villafranca, 1986) allow for specific replacement of each of the two tryptophans present in each subunit with spectroscopically silent residues, thus providing independent spatially separated fluorescent probes, while preserving the local structure surrounding a particular tryptophan. The combination of site-directed mutagenesis and time-resolved fluorescence spectroscopy provides a detailed description of the previously reported steady-state fluorescence properties of glutamine synthetase (Timmons et al., 1974; Meek et al., 1982).

The X-ray crystal structure of GS indicates that one tryptophan (Trp-57) lies near the outer edge of the hexameric ring in a peptide loop near the N-terminus (Almassy et al., 1986). The Trp-57 loop lies approximately 9.2 and 13.9 Å from the n1 and n2 metal binding sites, respectively. This has recently been confirmed for the solution structure with luminescence studies utilizing mutant proteins and Tb^{3+} bound to the metal sites (McNemar et al., 1990). The Trp-57 loop is characterized by large crystallographic *B* factors, and it has been proposed that flexibility in this region is essential for catalytic function (Yamashita et al., 1989; Almassy et al., 1986). In addition, the Trp-57 loop lies very close to the site of adenylylation (Tyr-397) in the adjacent subunit. This covalent modification provides a means of regulating the catalytic properties of the enzyme in vivo (Ginsburg et al., 1970), and it has been speculated that the Trp-57 loop may play a role in this regulatory mechanism (Almassy et al., 1986). The second tryptophan, Trp-158, is also contained within a loop, which projects inward toward the 6-fold axis of symmetry at the center of the rings (Figure 1). The Trp-158 loop has been implicated as a proteolytically sensitive region in vitro, and it has been suggested that binding of several allosteric inhibitors may provide protection from this proteolysis (Dantry-Varsat et al., 1979). Trp-158 lies on the opposite side of the active site approximately 16.9 and 9.5 Å from the metal binding sites (McNemar et al., 1990). Also, it has been shown that this loop may become ADP-ribosylated in vivo and may represent an additional site of regulatory importance (Moss et al., 1988). The results presented here indicate that these two tryptophans exhibit heterogeneous fluorescence decay kinetics. They are characterized by similar fluorescent lifetime components yet differ in their relative distribution of these discrete components. In addition, ATP binding results in a conformational change localized to the Trp-57 region, which appears to undergo a ligand-induced shift in the equilibrium distribution of the microconformational states present in this region of the protein.

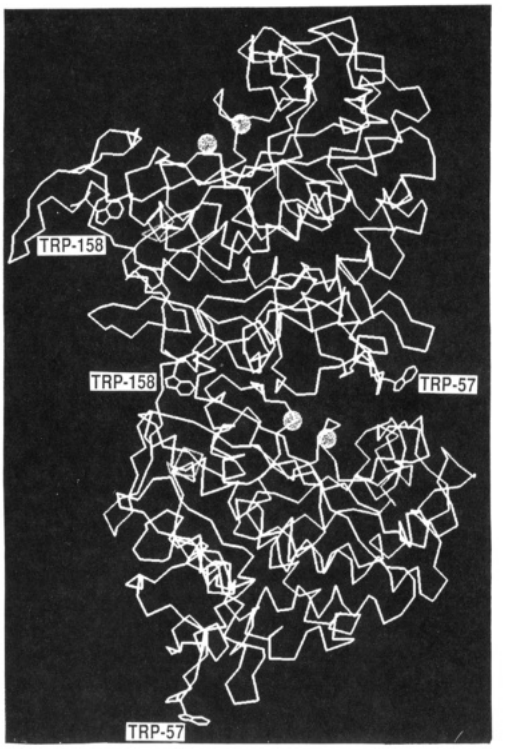

FIGURE 1: X-ray crystal structure of glutamine synthetase from *S. typhimurium*. The α-chains of two adjacent subunits are shown with the Trp-57 and Trp-158 indicated. The solid circles represent the two Mn^{2+} ions. The dodecamer exists as two face-to-face hexagonal rings where each hexamer contains three of the dimeric units shown here [see Almassey et al., (1986)].

Materials and Methods

Site-Directed Mutagenesis and Cell Growth. Site-directed mutagenesis was performed according to the method of Kunkel et al. (1985). This was accomplished by using single-stranded template obtained from a plasmid constructed by subcloning the *Eco*RI–*Hind*III fragment from the previously described pgln6 (Backman et al., 1981) into pTZ18 obtained from Amersham. Template was isolated from *E. coli* strain RZ1032 harboring this construction and coinfected with M13KO7 helper phage. After isolation of mutant clones, W57L enzyme was expressed in pgln35 by subcloning the *Bsu*I136–*Bgl*II fragment into pgln35. W158S enzyme was also expressed in pgln35 after construction by analogous methods. Both mutant plasmids were transformed into the *E. coli* strain YMC11, which contains a deletion in chromosomal glutamine synthetase (Backman et al., 1981). Wild-type protein was obtained from an overexpression system consisting of the strain YMC10 harboring the plasmid pgln35.

Protein Purification and Characterization. Wild-type and mutant GS was purified by the zinc precipitation method previously described (Miller et al., 1974). Several growths of the W57L mutant under conditions which typically afford GS of low adenylylation state resulted in the isolation of W57L

[1] Abbreviations: GS, glutamine synthetase; W57L, site-directed mutant which contains leucine in place of tryptophan at position 57; W158S, site-directed mutant which contains serine in place of tryptophan at position 158. Subscripts refer to the average adenylyation state of the protein.

which had an average adenylylation state of 10 or greater. Thus, in order to study the low adenylylation state of this enzyme, it was necessary to perform in vitro deadenylylation. This was accomplished by treatment of purified W57L with snake venom phosphodiesterase according to the method described by others (Shapiro et al., 1967). A protease inhibitor cocktail including phenylmethanesulfonyl fluoride (10^{-3} M final concentration) and pepstatin A (10^{-7} M) was used to inhibit potential proteolysis resulting from the commercially available snake venom phosphodiesterase (Sigma). After phosphodiesterase treatment, the mutant protein was repurified by zinc precipitation and ammonium sulfate fractionation according to the original purification procedure (Miller et al., 1974). This treatment typically resulted in a decrease in the average adenylylation state from greater than 10 to less than 3. The average state of adenylylation of the wild-type protein was determined by the γ-glutamyltransferase assay as described by Stadtman and Ginsburg (1974). The adenylylation state of the mutant proteins was determined from the extent of incorporation of ^{32}P from [α-^{32}P]ATP by adenylyltransferase as described elsewhere (Hennig & Ginsburg, 1971), with some modification in the assay procedure. After in vitro adenylylation with purified *E. coli* ATPase, solutions were pipetted onto small pieces of Whatman chromatography paper. The papers were washed several times with 5% TCA followed by washing with ethanol. The air-dried filters were counted for incorporation of ^{32}P into acid-precipitable material as described elsewhere (Walsh & Krebs, 1971). The adenylylation state determined by this method was confirmed by determination of inorganic phosphate released from acid hydrolysis.

Enzyme activities were determined by the standard γ-glutamyltransferase assay (Woolfolk et al., 1966) and by the biosynthetic assay as described by Kingdon et al. (1968). Briefly, this assay consists of a 1-mL solution containing 33 μg of pyruvate kinase and lactate dehydrogenase, 100 mM KCl, 0.19 mM NADH, 1 mM phosphoenolpyruvate, 50 mM NH_4Cl, and 0.5–3 mg of wild-type or mutant glutamine synthetase in 20 mM Hepes, pH 7.5. For determination of K_m's, the appropriate substrate was varied in concentration while the other substrates were ATP, 3 mM; glutamate, 50 mM; and $MgCl_2$, 25 mM. Assays were run at 37 °C where the change in absorbance at 340 nm was monitored, using an extinction coefficient for NADH of 6.22 mM^{-1} cm^{-1}.

Fluorescence Measurements. Steady-state fluorescence experiments were performed on either a Perkin-Elmer MPF44B or a MPF66 fluorescence spectrophotometer. Time-resolved fluorescence measurements were performed at the Laboratory for Fluorescence Dynamics, University of Illinois at Urbana—Champaign. The frequency response of the fluorescence emission was measured by using the cross-correlation phase and modulation fluorometer described by Alcala et al. (1987), with a harmonic content of 2-MHz pulses from a mode-locked Nd–YAG laser with the frequency doubled. This was coupled to a cavity-dumped dye laser (Models 7220 and 702) and to an external frequency doubler. Each of these components was obtained from Coherent Corp. The excitation wavelength was 295 nm and was set with a birefringent crystal of the dye laser. Phase and modulation data were obtained at 320, 330, 340, 350, and 380 nm except where otherwise noted. Monochromator slits were set at 2 mm (8-nm band-pass). *p*-Terphenyl in cyclohexane was used as a reference compound to correct for color shifts and instrumental phase delay. This reference has a lifetime of 1.06 ns. The error in the phase angles was less than 0.6° and of the demodulation factors was less than 0.004. Fluorescence measurements were performed in 20 mM Hepes, 100 mM KCl, and 3 mM $MnCl_2$, pH 7.4. Protein concentrations ranged from 10 to 20 μM.

Table I: Kinetic Parameters for Tryptophan Mutants

	assay, activity			
	transferase, pH 7.56	Mg^{2+} biosynthetic assay		
protein[a]	(units/mg)	units/mg	K_m(ATP) (μM)	K_m(Glu) (mM)
wild type 2.5	124 ± 9	42 ± 2	146 ± 13	4.0 ± 0.4
W57L 2.8	141 ± 9	18 ± 1	324 ± 21	9.0 ± 0.8
W158S 3.5	23 ± 4	2.4 ± 0.8	280 ± 14	9.8 ± 0.9

[a] Numbers refer to average adenylylation state.

The frequency domain multiwavelength data were analyzed by using the Global Analysis software package, Globals Unlimited (Knutson et al., 1983; Beecham et al., 1983; Beecham & Gratton, 1988). This analysis is based on the theories and algorithms of the Marquardt–Levenburg type with nonlinear least-squares analysis. The global analysis allows for the simultaneous fitting of multiple data sets. The analysis utilizes the relations: $\tan \phi = \omega\tau$ and $m = [B/A]/[b/a] = (1 + \omega^2\tau^2)^{-1/2}$, where $\omega = 2\pi \times$ frequency in hertz and τ is the lifetime of the excited state. Error analysis of the recovered lifetimes was performed by allowing a lifetime value to vary in an incremental fashion while allowing the remaining parameters to relax to new minima, and calculating the new χ^2. Decay-associated spectra were obtained by combining the time-resolved data with the steady-state emission spectra as described elsewhere (Philips et al., 1989).

Results

Characterization of Mutant Proteins. In order to ensure that the mutant proteins utilized here provide good models for the dynamic nature of the tryptophans of the native enzyme and the structural changes which take place when ligands bind, each of the mutant proteins was analyzed for catalytic activity based on the Mg-dependent biosynthetic assay (Kingdon et al., 1968) and the standard γ-glutamyltransferase assay (Woolfolk et al., 1966). In addition, the pH dependence of the proteins in the transferase assay was determined and found to be essentially identical for all three enzymes except for a sharper decrease in activity at pH's above 7.5 for the W158S mutant. The specific activities of these enzymes are summarized in Table I. Furthermore, the K_m values for Mg^{2+}, ATP, and glutamate were determined for the biosynthetic assay. This was especially important since, as pointed out below, the mutants demonstrated differential fluorometric sensitivity to ligand binding. Thus, it was necessary to demonstrate kinetically that comparable concentrations of ligands saturate the enzyme binding sites. As can be seen from Table I, the K_m values for ATP and glutamate with the mutant proteins are slightly higher than with the wild type. However, inspection of the saturation curves (not shown) obtained with varying concentrations of ATP clearly indicated that both mutants are completely saturated at the levels of ATP used in these studies (2 mM). Clearly, the W158S mutant demonstrates slightly diminished catalytic activity compared to the wild type GS but retains the ability to bind ATP and glutamate tightly. Since the results presented below demonstrate similarity in behavior between the wild-type and W158S proteins with respect to fluorescence measurements, it is reasonable to assume that the conformational dynamics and structural changes studied here closely resemble those of the wild-type protein. Furthermore, the lifetime distribution observed for Trp-57 is essentially identical with the wild type,

Table II. Global Analysis of Tryptophan Emission Data for Glutamine Synthetase

protein	exponential model tested, χ^2 single	double	triple	lifetimes recovered[a] (ns)	fractional intensity at 320, 330, 340, 350, 380 nm
wild type	205	11.4	1.569	4.53 ± 0.70/0.26	0.643, 0.671, 0.661, 0.662, 0.682
				1.94 ± 0.76/0.41	0.310, 0.288, 0.304, 0.310, 0.290
				0.31 ± 0.29/0.33	0.046, 0.041, 0.036, 0.029, 0.027
W158S	321	11.29	0.676	4.77 ± 0.54/0.08	0.699, 0.688, 0.672, 0.653, 0.620
				1.72 ± 0.79/0.23	0.262, 0.271, 0.286, 0.296, 0.320
				0.10	0.036, 0.041, 0.042, 0.048, 0.051
W57L	267	6.80	1.308	5.04 ± 2.46/0.70	0.229, 0.297, 0.351, 0.371, 0.379
				2.28 ± 0.21/0.62	0.658, 0.606, 0.573, 0.563, 0.552
				0.37 ± 0.13/0.22	0.113, 0.096, 0.088, 0.085, 0.075

[a] ± indicates the high and low limits of resolution at the 67% confidence interval based on rigorous error analysis as described under Materials and Methods.

suggesting that the structure of the W158S mutant is unaltered in the region of the Trp-57 loop.

Time-Resolved Fluorescence. Steady-state fluorescence studies of the mutant proteins immediately demonstrated a significant disparity in the relative contributions of the individual tryptophans to the fluorescence emission of the wild-type protein. Both tryptophans have essentially identical emission maxima when excited at 295 nm. Trp-57, however, emits approximately 3 times as much total emission intensity as Trp-158, suggesting that the steady-state fluorescence observed with the wild-type enzyme is dominated by Trp-57. Notably, Trp-57 is much more solvent-exposed than Trp-158, based on the X-ray crystal structure. In order to further differentiate the fluorescent properties of the individual tryptophans, the lifetime distributions of the three proteins were determined as a function of emission wavelength.

Wild-type $GS_{2.5}$ is best described as having a triple, discrete exponential decay scheme with recovered lifetime values of 4.53, 1.94, and 0.3 ns. The fractional intensities of these lifetime components are approximately 65%, 31%, and 4%, respectively. This was determined by global analysis of phase lag and modulation ratios determined at 12 modulation frequencies ranging from 2 to 200 MHz at 5 wavelengths spanning the emission spectrum 320, 330, 340, 350, and 380 nm. The phase and modulation data are shown in Figure 2. Global analysis was performed with the lifetimes constrained to remain the same at each wavelength and with the fractional intensities of each component allowed to vary. The data were fit to single, double, and triple discrete exponential decay schemes as well as to a continuous Lorentzian distribution model. As can be seen from Table II, the χ^2 value for the triple-exponential decay scheme is significantly lower than the alternative models; in fact, a χ^2 value of 1.57 indicates an excellent fit for an oligomeric protein with a natural source of heterogeneity resulting from a low level of adenylylation. The χ^2 values for the double- and single-exponential decay schemes are 11.4 and 205. It can be seen from the analysis utilizing the sum of three exponentials that there is very little wavelength dependence for any of the lifetimes and they are not resolved along the emission spectrum (Figure 2, Table II). In order to determine the experimental resolution of the recovered lifetimes, rigorous error analysis was performed as described under Materials and Methods. The errors associated with the recovered lifetimes are summarized in Table II. The three lifetimes are clearly resolved from each other, although the long-lifetime and the median-lifetime are not as well resolved on the long-lifetime side, and may be as high as 5.23 and 2.70 ns at the 67% confidence level. The wild-type enzyme is dominated by this long-lifetime component which provides approximately 60% of the total emission intensity. The data were also analyzed in terms of a continuous Lorentzian distribution of lifetime components. It is clear that many systems are most accurately described by nondiscrete, continuous distributions of tryptophan emissions (Alcala et al., 1987). When the phase and modulation data obtained for the wild-type protein are analyzed as a single Lorentzian distribution, the χ^2 value is 38.3 with the recovered lifetimes centered at 4.72 ns. When a trimodal Lorentzian distribution is tested, the χ^2 value improves significantly to 3.12 with lifetimes centered at 4.80, 2.56, and 0.62 ns. It is very noteworthy that each of the component distributions within this analysis is very narrow (width = 0.04). Thus, there is not only a significant improvement in the χ^2 value when fit to a sum of discrete exponentials but also the distribution model which gives the best fit is characterized by very sharp distributions. This may indicate that even if the tryptophans contained in GS are distributed among a spectrum of orientations, the rate of interconversion between the highly populated conformational substates is fast or that the majority of tryptophan residues

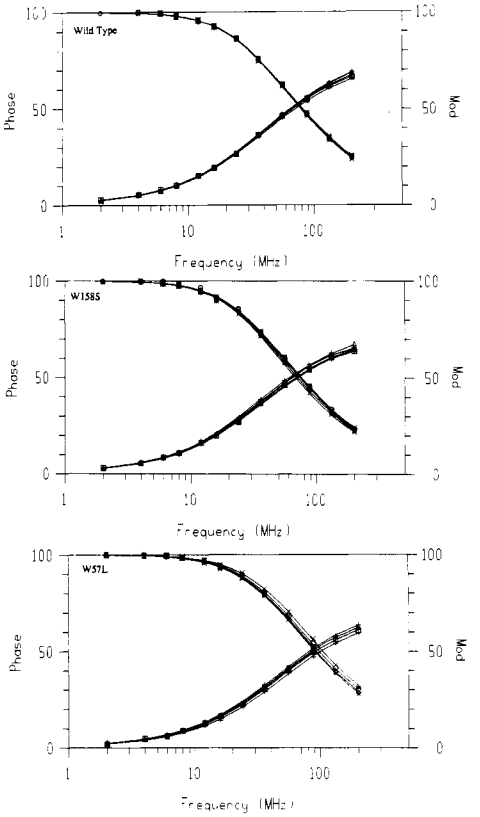

FIGURE 2: Multifrequency phase and modulation data for the wild-type and mutant proteins. The phase and modulation data for five wavelengths are shown: 320, 330, 340, 350, and 380 nm. The top panel is wild type, the middle panel is W158S, and the bottom panel is W57L.

exist in one of the three microconformational states obtained with the discrete analysis. Therefore, we have chosen to consider GS in terms of discrete lifetime components.

Similar analysis with W158S $GS_{3.5}$ yielded χ^2 values of 321, 11.29, and 0.676 when fit to a single, double and triple discrete exponential decay scheme. Attempts to fit the decay of this mutant to a single Lorentzian distribution model and a trimodal distribution resulted in χ^2 values of 39.7 and 4.62, respectively. The lifetime values and fractional intensities of the various components recovered from the discrete analyses are summarized in Table II along with the data obtained with the wild-type protein. As with the wild-type enzyme, a three-component model best describes the W158S mutant, with recovered lifetime values of 4.77, 1.72, and 0.10 ns. Also, there is very little wavelength dependence for any of the lifetimes, as was observed with the wild type, although the longer lifetime is very slightly blue-shifted compared to the median lifetime. The fractional intensities of the lifetimes are very similar to those found for the wild type except there is an even greater proportion of the long-lifetime component. Rigorous error analysis demonstrates that the lifetimes are clearly resolved from one another but in this independent analysis they are not resolved from the lifetime values recovered for the wild type (Table II).

The fluorescence emission decay kinetics of the W57L mutant, which retains tryptophan at position 158, are also best described by a triple-exponential decay. The χ^2 value increases substantially when the phase and modulation data are fit to single- or double-exponential decay models, whereas a triple-exponential decay scheme is fit well by the data with a χ^2 of 1.31. As with the other two proteins, when the phase and modulation data are fit to Lorentzian distribution models the χ^2 values increase substantially. These χ^2 values are 46.2 and 5.24 for unimodal and trimodal Lorentzian distributions, respectively. The recovered lifetimes obtained with the discrete, three-component model (5.04, 2.39, and 0.37 ns) are nearly identical with the wild-type and W158S proteins, and a significant wavelength dependence is strikingly absent (Table II). It is interesting that in opposition to Trp-57, Trp-158 has a slightly red-shifted long-lifetime component. The lifetime components are readily resolved from each other but not from the lifetimes recovered from the wild-type and W158S enzymes. It is noteworthy that error analysis yields significantly broader confidence limits (67%) than observed with the wild-type and W158S proteins. In particular, the long-lifetime component is not well resolved on the long-lifetime side of 5.04 ns, and may be as high as 7.56 ns. Also, the median lifetime is less well resolved on the shorter side of 2.28 ns, and may be as low as 1.21 ns. We presume that this increase in the uncertainty associated with the recovered lifetimes results from the low level of fluorescence emission of the W57L mutant. There is, however, an obvious difference in the relative intensities of the components which are present, compared to the wild-type and W158S proteins. With the W57L species, the median lifetime provides as much as 60% of the fractional intensity with the long lifetime providing only 38%. This distribution is inverted from that observed with the wild type and W158S mutant. As with Trp-57, Trp-158 appears to be characterized by a sum of three discrete components with lifetimes near 0.5, 2, and 5 ns. Thus, the individual tryptophan residues of wild-type Mn^{2+}–GS are not uniquely distinguished by resolvable lifetime components or by spectrally resolved lifetime species. However, the two tryptophans appear to be distinguishable by significantly different distributions of nearly identical lifetime components.

As pointed out above, it appears that the lifetime distribution observed with the wild-type enzyme is dominated by Trp-57. We cannot determine whether the lifetime values for the tryptophan in the W158S mutant are actually identical with those recovered for the wild type, but they are not resolvable with the data obtained in these studies. This was tested directly by combining data from the wild-type and W158S proteins and performing global analysis when different linkage schemes are used to constrain different sets of parameters. When all three lifetimes are constrained to remain the same for both proteins, at each wavelength, and the fractional intensities are allowed to vary independently, the resulting χ^2 value is 3.42, and the recovered lifetimes are 4.85, 2.14, and 0.21 ns. The fractional intensities range from 70% to 59% for the long-lifetime component, 33% to 39% for the median-lifetime component, and 2.7% to 5.7% for the short-lifetime component. The combined analysis affords a nearly identical lifetime distribution and recovered lifetime values as the individual analyses. When the same data sets are analyzed with a less stringent linkage scheme in which only the long-lifetime value is constrained to remain the same for the two proteins, the χ^2 value increases to 5.08. When the short- and median-lifetimes values are constrained to be the same for both proteins, the χ^2 value is 4.48. Comparison of these analyses and the number of linked parameters in each case suggests that the model in which all three sets of lifetime components are treated as if they were identical for both proteins is the best description of the data obtained. It is clear that each tryptophan of glutamine synthetase displays heterogeneous decay kinetics and that both tryptophans have lifetime components which are nearly identical. In particular, the components recovered for Trp-57 are best fit to a model in which they are considered as identical with the components recovered for the wild-type protein.

ATP Binding. It has been extensively documented that ATP binding results in a dramatic enhancement of the tryptophan emission of glutamine synthetase (Timmons et al., 1974; Meek et al., 1982). In order to determine whether the effect of ATP binding can be attributed specifically to either of the two tryptophans, ATP complexes of the mutant proteins were investigated. Steady-state experiments demonstrated that at pH 7.4 ATP causes a 1.6–1.7-fold enhancement of the emission amplitude with a very small blue-shift in the emission maximum from 332 to 330 nm. With the W158S protein, there is a nearly identical increase in amplitude and shift in emission maximum induced by ATP. In contrast, saturating levels of ATP produced no enhancement of the fluorescence intensity for the W57L mutant enzyme. As pointed out above, this lack of enhancement does not appear to be attributable to destruction of the ATP binding function of this mutant. This mutant is as active as the wild-type protein in the γ-glutamyltransferase assay and is saturated by comparable concentrations of ATP in the biosynthetic assay (Table I). Together these observations suggest that the previously documented change in intensity caused by ATP is localized to alteration of the fluorescence of Trp-57, with only a very small change at Trp-158. To obtain more detailed information, phase and modulation experiments were performed with the ATP complexes of all three enzymes.

For the wild-type enzyme, fluorescence data with the ATP complex are best fit by a triple-exponential decay with resolved lifetime components that are essentially identical with those found in the unliganded state. However, it is apparent that the fractional intensities of these individual components have changed compared to the unliganded state such that the

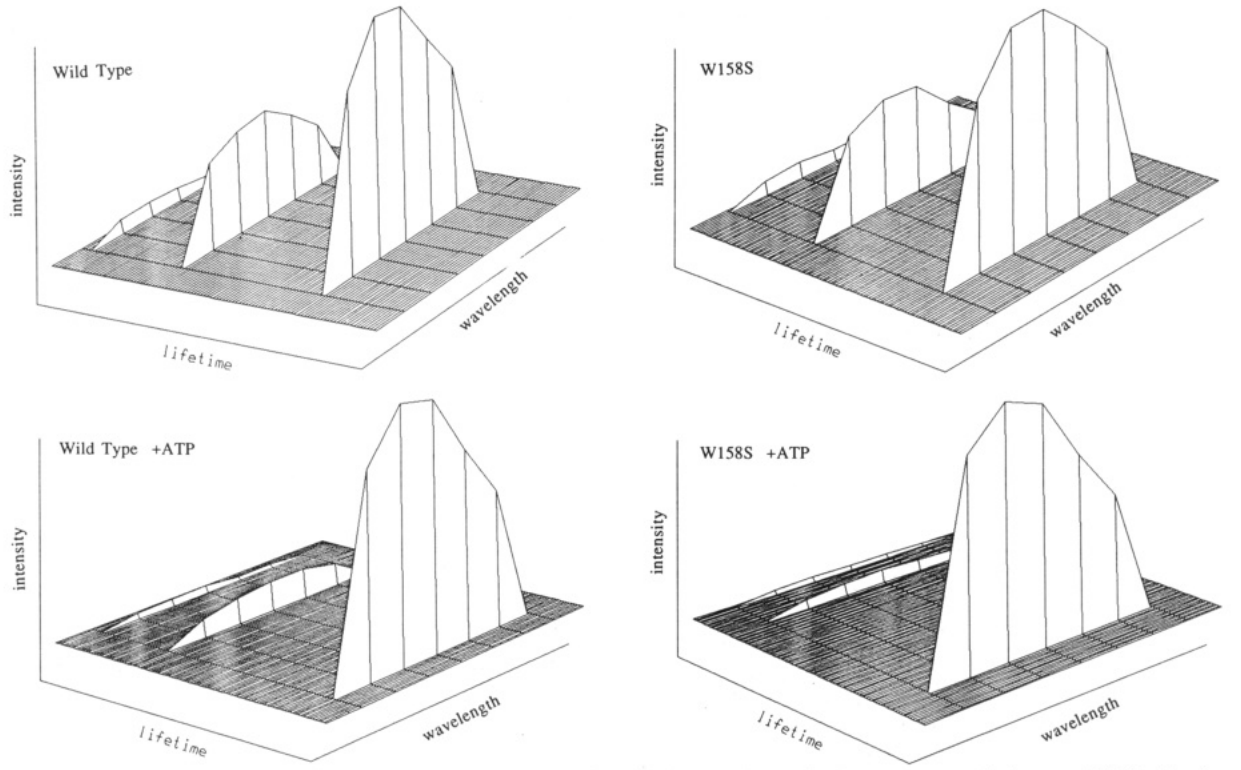

FIGURE 3: Decay-associated spectra of the wild-type and the W158S glutamine synthetase in the presence and absence of ATP. In the model which is illustrated, ATP causes a nearly identical redistribution of the existing lifetime components for both proteins. The lifetime values do not change. The lifetime values correspond to components of approximately 5, 2, and 0.5 ns. Left panel: wild type. Right panel: W158S.

long-lifetime component (4.46 ns) is nearly 80% of the total intensity, and the median-lifetime component (1.87 ns) is diminished to about 15%. This effect is slightly enhanced with the W158S mutant. When the individual lifetime components are not constrained to remain the same for the different ligand states, the lifetime components do not change, within the resolution of the data, but the relative fraction of the long-lifetime component becomes nearly 90% of the species present when ATP is bound. The results from this global analysis are summarized in Table III. Rigorous error analysis indicates that the lifetime components do not change upon addition of ATP. When the combined data for the wild-type enzyme in the presence and absence of ATP are analyzed with the lifetime values linked across ligand state and with the fractional intensities allowed to vary, a χ^2 value of 2.53 is obtained. The recovered lifetimes values are 4.61, 1.97, and 0.23 ns, and the fractional intensities change in a similar fashion as the other linkage schemes. Similarly, for the W158S mutant, when the lifetime components are constrained to remain the same in the presence and absence of ATP, the χ^2 value indicates a slightly better fit, $\chi^2 = 1.72$, with recovered lifetime values of 4.84, 1.73, and 0.18 ns. Thus, the phase and modulation data for the wild-type enzyme and the W158S mutant are best fit to a model in which the lifetime values in the absence of ATP are the same as the recovered lifetime values in the presence of ATP, but the fractional intensities change. This hypothesis is examined with additional linkage schemes below. Since it is physically possible that the ATP complex of GS may be characterized by a distribution of lifetimes rather than a sum of discrete components, it was necessary to fit the data for the ATP complex to a Lorentzian model, as was done with the substrate-free protein. The χ^2 values for a unimodal and trimodal Lorentzian distribution are 38.8 and 18.1, respectively. Thus, it appears that like the ligand-free protein, the ATP complex is best described by a sum of three lifetime components. The similarity in spectral changes observed with addition of ATP to the wild-type and W158S mutant enzymes is best demonstrated by comparison of the decay-associated spectra, which are obtained by combining the time-resolved data and the steady-state spectra. The resulting spectra represent those expected for the individual components assuming they behave as noninteracting excited states. The normalized decay-associated spectra for ligand-free and ATP complexes of the wild-type and W158S enzymes are compared in Figure 3. The similarity between the two proteins is striking. The effect of ATP binding is slightly attenuated for the wild type, presumably due to a minor contribution from Trp-158 which does not change significantly when the ligand is added, as discussed below.

The lack of a significant effect on the steady-state spectrum when ATP binds to the W57L enzyme would suggest that the lifetime distribution of Trp-158 does not change due to binding of this ligand. In an attempt to detect ATP-induced changes in this tryptophan residue, the lifetime components were determined with a 305-nm emission cuton filter in the presence and absence of ATP. Use of the emission filter instead of the monochromator provides a larger total emission intensity and thus provides greater sensitivity. It was essential to demonstrate that the ATP-induced change which is observed with the wild type is still detectable when the filter is used to replace the emission monochromator. The shift toward a larger fraction of the longer lifetime component is still apparent with the wild type, as was observed when using the monochromator. By comparison, the W57L mutant demonstrates little change when ATP is added, although there is a very small shift toward longer lifetimes in the modulation data. The phase angles are essentially superimposable in the presence and absence of ATP (not shown). The experiment demonstrates that the W57L mutant is only slightly affected when ATP binds under these conditions. As a result, we have focused on a direct comparison between the fluorescence changes observed with the wild-type protein and those seen with the W158S mutant.

Table III: Combined Global Analysis for Wild Type ± ATP and W158S ± ATP

protein ligand	χ^2	lifetime (ns)[a]	fractional intensity at 320, 330, 340, 350, 380 nm
WT, −ATP	2.78	4.46 ± 0.57/0.41	0.689, 0.685, 0.680, 0.681, 0.701
		1.87 ± 0.71/0.24	0.272, 0.279, 0.287, 0.292, 0.274
		0.242 ± 0.61/0.19	0.039, 0.034, 0.033, 0.026, 0.025
WT, +ATP		5.41 ± 0.20/0.15	0.889, 0.875, 0.856, 0.846, 0.662
		1.87 ± 0.69/0.03	0.090, 0.103, 0.131, 0.0.134, 0.138
		0.24 ± 0.46/0.23	0.021, 0.023, 0.021, 0.019, 0.044
W158S, −ATP	1.75	4.74 ± 0.80/0.08	0.628, 0.661, 0.680, 0.696, 0.707
		1.72 ± 0.90/0.22	0.315, 0.285, 0.273, 0.258, 0.250
		0.19 ± 0.80/0.19	0.056, 0.054, 0.047, 0.0046, 0.043
W158S, +ATP		5.22 ± 0.73/0.63	0.926, 0.921, 0.915, 0.905, 0.896
		1.71 ± 0.46/0.31	0.051, 0.055, 0.062, 0.070, 0.077
		0.19 ± ND[b]	0.023, 0.024, 0.023, 0.025, 0.027

[a] Errors reported for the lifetimes are the high and low limits at the 67% confidence level as determined from rigorous error analysis. [b] Not determined.

By combining data sets from the two proteins in the presence and absence of ATP, and utilizing a variety of linkage schemes to constrain different parameters, we have attempted to determine whether the data are most consistent with a model in which any lifetime components change when ATP binds, whether only their fractional intensities change, or both. Here the term "linkage" indicates that parameters are constrained to remain the same. When the data for the wild type in the presence and absence of ligand are combined with the data for the W158S mutant, several linkage schemes may be envisioned. When the median- and short-lifetime components are linked for both proteins and ligand states, and the long-lifetime component is constrained to be the same for the wild type and mutant in the absence of ATP and independently constrained to be the same for both proteins in the presence of ATP (53 linkages, 114 parameters), the χ^2 value is 2.54. For this model, which tests whether the long-lifetime value changes when ATP is added, and assumes that the lifetime values are the same for both proteins, the recovered lifetime values are 0.44 ns for the short component, 2.26 ns for the median component, 4.90 ns for the long component in the absence of ATP, and 5.31 ns for the lifetime in the presence of ATP. These are nearly identical with the lifetime values obtained with the other linkage schemes which allow either the median- or the long-lifetime components to vary between ligand states. This model tests the possibility that the median and short lifetimes are unaffected by ATP binding. When the median lifetime is linked in a similar fashion to test the possibility that the median component changes when ATP binds, the χ^2 value is 2.43. The lifetime values obtained from this model are 5.21 ns for the long component, 0.47 ns for the short component, 2.52 ns for the median component in the absence of ATP, and 1.46 ns for the median-lifetime component in the presence of ATP. Most importantly, when all three lifetime components are constrained for each protein and ligand state, and only the fractional intensities are allowed to vary (54 linkages, 114 parameters), the χ^2 is not raised significantly, $\chi^2 = 2.57$, even though there is an additional constraint on the fitting parameters. Thus, allowing either the median-lifetime value or the long-lifetime value to vary with the presence or absence of ATP does not improve the fit of the data to the model tested. Furthermore, when either the long-lifetime component or the median-lifetime component is allowed to vary between ligand states, the recovered values are not resolved by rigorous error analysis. On the basis of these analyses, we propose that ATP binding does not result in the population of new conformational states characterized by different lifetime components but that ATP simply causes an alteration in the relative contribution of the lifetime components which are already present. Taken together, these data are consistent with a model in which Trp-57 undergoes a redistribution of the relative population of the three distinguishable microconformations when ATP binds. We acknowledge the possibility that ATP binding does actually result in the presence of new microconformations which were not present in the absence of ligand and that new states are coincidentally identical in their characteristic lifetime values with those present without ATP.

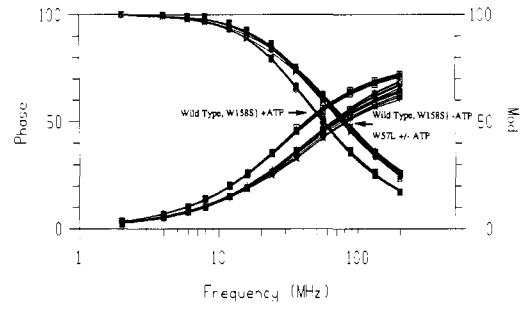

FIGURE 4: Phase and modulation data for combined global analysis including three proteins in the presence and absence of ATP. The frequency response of the wild type and the W158S mutant is shifted to lower frequencies in the presence of ATP. The phase angles and modulation ratios for the wild type and the W158S mutant are shown for five wavelengths spanning the emission. For the W57L mutant, the data obtained with a 305-nm cuton emission filter are included.

In order test how well the phase and modulation data fit the proposed model, a combined total global analysis was performed with data from all three proteins in the presence and absence of ATP. For the W57L mutant, the data obtained with emission filter were included. The lifetime components were constrained to be the same for the wild-type and the W158S enzymes in both ligand states, and the fractional intensities were allowed to vary for all three proteins. The lifetime components for the W57L mutant were also constrained to remain the same within each ligand state but were allowed to vary from the lifetime components of wild-type and W158S enzymes. This analysis is summarized in Table IV, and the phase and modulation data are shown in Figure 4. The χ^2 value for this model, which has 22 individual data sets, is 2.48. It is clear that both the wild type and the W158S mutant are driven to a larger proportion of the long-lifetime component when ATP binds. The W57L enzyme is not affected by ATP, within the resolution of our data. The phase and modulation data for the W57L mutant in both ligand states are "buried" within the data for the wild type and the W158S mutant in the absence of ATP. It is necessary to reiterate the difference in the analyses presented in Tables III and IV. In the analysis shown in Table III, the lifetime

Table IV: Combined Global Analysis for Wild Type and Mutants ± ATP

protein	ligand	lifetime (ns)	fractional intensity at 320, 330, 340, 350, 380 nm
wild type	-ATP	5.32 ± 0.20/1.10	0.422, 0.443, 0.431, 0.426, 0.446
		2.62 ± 0.29/0.25	0.541, 0.491, 0.508, 0.522, 0.506
		0.49 ± 0.14/0.15	0.077, 0.066, 0.061, 0.052, 0.048
wild type	+ATP	5.32	0.887, 0.869, 0.839, 0.831[a]
		2.62	0.088, 0.127, 0.033, 0.042
		0.49	0.039, 0.033, 0.42, 0.042
W158S	-ATP	5.32	0.427, 0.468, 0.485, 0.502, 0.518
		2.62	0.459, 0.426, 0.420, 0.407, 0.396
		0.49	0.114, 0.106, 0.095, 0.091, 0.086
W158S	+ATP	5.32	0.894, 0.889, 0.880, 0.867, 0.858
		2.62	0.068, 0.071, 0.080, 0.090, 0.096
		0.49	0.038, 0.040, 0.040, 0.043, 0.046
W57L	-ATP	8.85 ± 1.9/1.6	0.201
		2.83 ± 0.57/0.60	0.702
		0.40 ± 0.30/0.40	0.097
W57L	+ATP	8.85	0.201
		2.83	0.649
		0.40	0.105

[a] Data for 340 nm are not included in this set of wild-type measurements. The confidence limits resulting from rigorous error analysis are the same for the different ligand states of the wild type and W158S, and they are the same for the different ligand states of W57L.

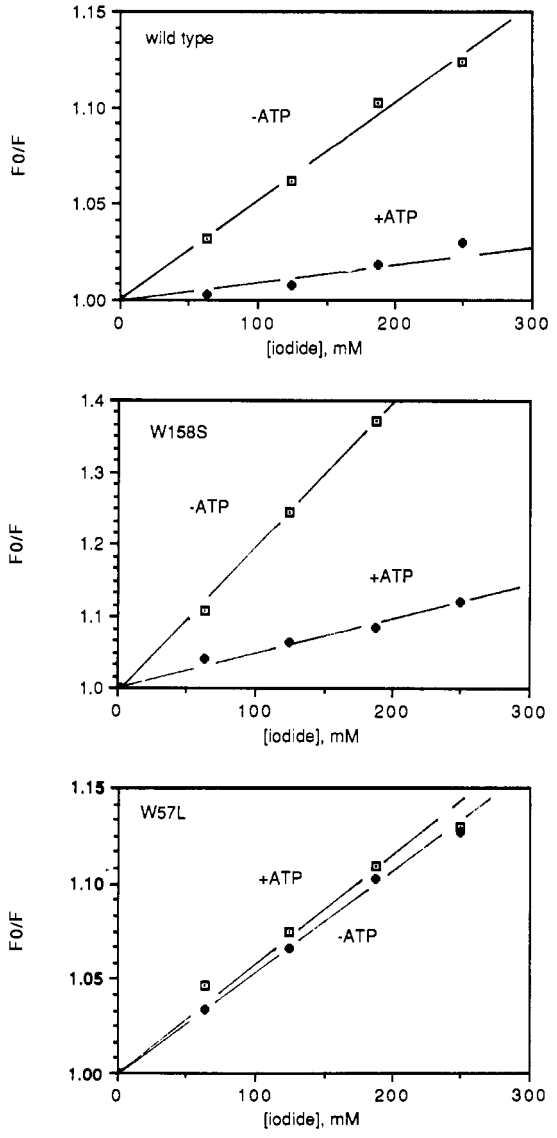

FIGURE 5: Steady-state Stern–Volmer plots for wild-type and mutant GS in the presence and absence of ATP. The concentrations of iodide are 0, 62, 125, 185, and 250 mM. The top panel is wild type, the middle panel is W158S, and the bottom panel is W57L.

components for the presence and absence of ATP have been allowed to vary for both the wild-type and the W158S enzymes. Although the recovered lifetimes are slightly different when ATP is added, they are not resolved from the recovered lifetime values in the absence of ATP based on rigorous error analysis. The data are fit equally well to an analysis when the lifetime components are constrained to remain the same in the presence and absence of ATP. Therefore, when the data from all three proteins are combined, as in Table IV, we have linked the lifetime components between ligand states for the wild type and linked these to the lifetime components for the W158S mutant.

Iodide Quenching. In order to further probe the physical nature of the individual lifetime components, we have performed solute quenching studies with the ionic quencher iodide in the presence and absence of ATP. Steady-state quenching studies clearly indicate a protection from iodide quenching when ATP is added to the wild-type protein. This effect is observed with W158S mutant as well, but is not apparent with the W57L mutant. The Stern–Volmer plots for the three proteins in different ligand states are shown in Figure 5. For four concentrations of iodide in samples kept at constant ionic strength with appropriate additions of KCl, there is a 3.0–3.5-fold decrease in the apparent Stern–Volmer quenching constant in the presence of ATP when linear regression is performed and the slopes from the plots are compared as K_{sv}, where $F_0/F = 1 + K_{sv}[I^-]$ and $[I^-]$ is the concentration of KI. Although the data fit well to a linear Stern–Volmer plot, careful inspection of the curves suggests possible deviation from linearity. This may result from a mixed population of fluorophores which differ significantly in their individual susceptibility to quencher. We note that the apparent quenching constants are higher for the W158S protein than for the wild-type enzyme and the W57L mutant. The apparent Stern–Volmer quenching constants are 0.46, 1.90, and 0.51 M^{-1} for the wild-type, the W158S, and the W57L enzymes, respectively, in the absence of ATP. It is not readily apparent why the W158S mutant demonstrates a greater sensitivity to iodide than the wild type, since the wild-type emission is largely due to Trp-57. If this decrease in the K_{sv} of the wild-type protein relative to the W158S mutant were simply due to the contribution of Trp-158, then it would be expected that the wild type would demonstrate a sensitivity to iodide that was intermediate between the two mutants. The steady-state data indicate that the K_{sv} values for the wild-type and W57L proteins are nearly identical. Since iodide is typically considered to quench fluorophores which are solvent-accessible

Table V: Global Analysis of Iodide Quenching for Wild-Type and W158S Glutamine Synthetase

protein	χ^2	lifetime (ns)	apparent K_{sv} (M^{-1})
wild type	2.79	5.46	0.16
		2.88	0.88
W158S	4.43	5.60	0.19
		2.48	1.81

or which lie near positive charge, these results suggest that when ATP binds, Trp-57 becomes less solvent-exposed or more embedded within the hydrophobic protein matrix [see Lakowicz (1983) and references cited therein]. It is possible that the effect of ATP results from the negative charges associated with the phosphoryl oxygens. If ATP were to bind with these oxygens next to Trp-57, then the negatively charged iodide would be expected to be ineffective as a quencher of this residue. If this is the case, then the results suggest that Trp-158 is not affected in a similar manner. These considerations are elaborated under Discussion.

We have also performed phase and modulation measurements in the presence of several concentrations of iodide. In contrast to the steady-state experiments which were conducted with constant ionic strength, the time-resolved measurements utilized a single sample with increasing concentrations of KI. Therefore, it was necessary to determine whether there were any ionic strength effects on the fluorescence of glutamine synthetase. In fact, for both wild-type and W158S proteins, the quenching which is observed with incremental addition of KI may partially be attributed to ionic strength increase (data not shown). Approximately 10% and 13%, respectively, of the total decrease in fluorescence intensity which is observed when iodide is added to the W158S and wild-type proteins may be attributed to this change in ionic strength. Still, it is clear that the quenching which is observed with KCl is a small fraction of that caused by KI and that the fluorescence intensity is only slightly affected by increasing ionic strength compared to increasing KI concentration. The recovered lifetime values, K_{sv}'s, and the calculated biomolecular quenching constants are summarized in Table V. For these measurements, the emission monochromator was set at 330 nm. Global analysis was performed with Stern–Volmer quenching constants applied to the median- and long-lifetime components. For these quenching experiments, the data were analyzed in amplitude space; i.e., the equations are solved explicitly in terms of the preexponential factors, α_i, rather than the fractional intensities, $f_i = \alpha_i\tau_i/\sum\alpha_i\tau_i$. The lifetimes and the apparent Stern–Volmer constants for the individual components were constrained to remain the same for the various iodide concentrations. The resulting lifetime in the absence of quencher, τ_0, was utilized with the apparent quenching constant, K_{sv}, to calculate the actual biomolecular quenching constant from the relation $K_{sv} = \tau_0 k_q$. The data (not shown) clearly indicate a dependence of the phase angles and modulation ratios on quencher concentration, and the global analysis indicates that the median-lifetime component is selectively quenched, with the long-lifetime component demonstrating much less susceptibility to quenching by iodide. This global analysis affords apparent bimolecular quenching constants of 2.9×10^7 and 3.1×10^8 M^{-1} s^{-1} for 5.46- and 2.88-ns lifetimes, respectively. A similar experiment with the W158S mutant reveals a nearly identical result. The bimolecular quenching constants are 3.5×10^7 and 7.3×10^8 M^{-1} s^{-1} for 5.60- and 2.48-ns lifetime components, respectively. As was observed with the steady-state experiments, the W158S mutant appears to be slightly more sensitive to quencher. It is striking that the median-lifetime component is much more sensitive than the long-lifetime component. The steady-state quenching data obtained with the wild-type protein and the W158S mutant are consistent with the phase and modulation quenching experiments. Since the quenching observed with the wild-type protein contains a contribution from Trp-158 for both the median- and long-lifetime components, the quenching constants for the individual lifetime components of the wild type would be expected to be less than those for the W158S mutant. Presumably, both the median- and long-lifetime components of Trp-158 are much less sensitive to iodide quenching than the long-lifetime component of Trp-57 (W158S). This has been experimentally observed (Atkins and Villafranca, unpublished results). These results are exactly what would be expected from the steady-state experiments in which ATP afforded protection from quencher. As demonstrated above, ATP causes the lifetime components to redistribute to a higher fraction of the long lifetime. Since this lifetime component is less sensitive to iodide quenching, addition of ATP results in the observed protection from quencher. These results suggest that the long-lifetime component may be characterized by a less polar, less solvent-accessible environment compared to the median-lifetime component.

Discussion

The combination of site-directed mutagenesis and time-resolved fluorescence spectroscopy has provided a detailed description of the dynamic nature of the individual tryptophans of *E. coli* glutamine synthetase. The results presented here suggest several important conclusions concerning the conformational states of the regions of the protein containing the Trp-57 loop and the central loop. Each of these regions of the protein has been implicated in catalysis and/or regulation of enzyme activity (Yamashita et al., 1989; Almassey et al., 1986). The steady-state fluorescence spectra of the mutant proteins suggest that the fluorescence emission of the wild-type enzyme is dominated by Trp-57. This has significant implication for the previously documented changes in the steady-state fluorescence intensity induced by various ligands including ATP, glutamate, ADP, the transition-state analogue L-methionine sulfoximine, and the allosteric effectors alanine and glycine. Clearly, the results presented here demonstrate that ATP binding has a dramatic effect on Trp-57. It remains to be determined whether each of these other ligands produces a structural change confined to this tryptophan or whether Trp-158 is also affected. Furthermore, steady-state fluorescence experiments indicate that the magnitudes of the fluorescence changes induced by ligands are dependent on pH and whether the enzyme is bound with Mg^{2+} vs Mn^{2+}. Obviously it is desirable to characterize the dynamics of the tryptophans of glutamine synthetase with several variations of metal ion, pH, and adenylylation state in order to understand the vastly different catalytic properties of the enzyme under different conditions. Such experiments are in progress. We have chosen to begin this characterization with the unadenylylated, Mn-bound enzyme in order to maximally utilize the available crystal structure as a model.

Both Trp-57 and Trp-158 exhibit multiexponential fluorescence decay kinetics. This is becoming a common observation for single-tryptophan-containing proteins (Royer et al., 1989; Hutnik & Szabo, 1989), although there are clearly examples of homogeneous, single-exponential decay (Hutnik & Szabo, 1989a,b). The source of the heterogeneity may include several physical phenomena including ground-state microheterogeneity, excited-state reactions, or excited-state proton transfer, and exciplex formation. In addition, considerable discussion has focused on whether tryptophan

fluorescence in proteins should be described by continuous distributions or discrete components (Alcala et al., 1987; Hutnik & Szabo, 1989). GS is best fit to a model described by three discrete components for both tryptophans. Since no analyses performed here yielded negative preexponential factors and since we have found no evidence for "red-edge effects" in the emission of either tryptophan residue, we do not expect excited-state reactions or solvent relaxation to contribute to the fluorescence decay kinetics of these tryptophans (Lackowicz, 1983). We have interpreted our results in terms of ground-state heterogeneity.

Trp-158 of *E. coli* glutamine synthetase is characterized by individual lifetime components that are unresolved from those found with Trp-57. Similar lifetime values are found with the wild-type protein. In addition, there is very little wavelength dependence for any of the lifetime components associated with either tryptophan. There is, however, a significant difference in the distribution of these lifetime components. Whereas Trp-57 is predominantly found in a conformation with a 5-ns lifetime, Trp-158 is dominated by a 2-ns lifetime with a smaller fraction of the longer component. It is nearly impossible to interpret the difference in fractional intensities observed for different lifetime values in terms of their physical environment, without additional experimentation. This has been successfully done for Trp-57 by observing the effects of the substrate ATP, and with the use of the ionic quencher iodide. It is clear from these studies that ATP affects a dramatic change in the conformational distribution associated with the lifetime components of Trp-57. This change appears to be largely localized to this region of the protein, under these conditions. It is important to point out, however, that this may include structural changes in the C-terminus of the adjacent subunit, near the site of adenylylation, which lies within a few angstroms of the Trp-57 loop in the absence of ATP (Almassey et al., 1987; Yamashita et al., 1989). On the basis of the results observed with the W57L mutant, ATP-induced structural changes at the inner diameter of the hexameric ring are very small or nonexistent.

It is especially noteworthy that ATP does not result in the recovery of new lifetime components but simply causes a shift in the relative distribution of the existing lifetimes. This model assumes that the ATP does not actually cause new conformations to be adopted which coincidentally have lifetime components that are unresolvable from those present in the absence of ATP. Thus, it appears that ATP does not stabilize a conformation of the Trp-57 loop which was previously not populated. Instead, ATP shifts the equilibrium distribution of conformational states to nearly completely favor one structure. It is important to distinguish between ligand-induced redistribution of conformational states and spectroscopic changes which may be caused by direct interaction between the ATP moiety and a given tryptophan. Although the crystal structure of the ATP complex is not available, it is reasonable to speculate that ATP binds near the n2 metal site (Almassey et al., 1986), and in fact it has been demonstrated that the ATP analogue 5′-[*p*-(fluorosulfonyl)benzoyl]adenosine covalently labels Lys-47 which lies within the Trp-57 loop (Pinkofsky et al., 1984). The steady-state data alone are insufficient to differentiate between a conformational redistribution and a direct interaction between ATP and fluorophore. However, a direct interaction would be expected to alter the lifetimes of the excited state or change the wavelength dependence of one or all of the individual components. As no change in lifetime values or the wavelength dependence of the decay-associated spectra of the individual components is observed, we propose that the observed effects of ATP binding reflect a change in the conformational equilibria of the Trp-57 loop.

The iodide quenching experiments indicate that the lifetime components observed with Trp-57 of glutamine synthetase are associated with different physical environments characterized by differential susceptibility to iodide. As expected for iodide, the decrease in lifetime as quencher concentration is increased indicates a dynamic quenching mechanism. Although it is possible that the heterogeneous emission kinetics observed for the individual tryptophans arise from other sources, the quenching experiments lend support to the proposal that this heterogeneity reflects ground-state microconformational heterogeneity. The large differences in bimolecular quenching constants which are observed for the individual lifetime components would not be expected unless the physical environment of these components differed significantly. With the aid of the X-ray crystal structure, it is possible to speculate about the difference in sensitivity to iodide quenching which is exhibited by the two tryptophans. Trp-57 lies within a loop connecting strands which run through the active site. In the immediate vicinity within this loop there are several residues which would not be expected to affect sensitivity to ionic quenchers, including several glycines. There is, however, a lysine residue directly adjacent to Trp-57 which would be expected to enhance iodide quenching. Also, several arginine residues are close to this tryptophan including Arg-339 and Arg-359 which lie within 5–8 Å of Trp-57, and may additionally enhance susceptibility to quenching by iodide. Furthermore, this loop is exposed to bulk solvent and is apparently easily accessible to small molecule/ion solutes. In contrast, access to Trp-158 is significantly more hindered, primarily as a result of close interactions between part of the central loop of one subunit with an α-helix in the same subunit (Figure 1). Residues near this tryptophan include both negatively and positively charged amino acids, so it is not readily apparent whether the ionic environment of Trp-158 strongly affects iodide quenching.

It is interesting to consider the results obtained with the Trp-57 loop of glutamine synthetase in light of the recent interest concerning the putative "phosphate gripper" role of flexible loops found in other nucleotide binding proteins (Pompliano et al., 1990; Wierenga et al., 1986). In several nucleotide binding proteins, a consensus sequence containing either Gly-X-Gly-X-X-Gly-Lys or Gly-X-X-X-X-Gly-Lys has been found in loop structures which have been implicated in binding to the pyrophosphate moiety of nucleotides. Recently, direct evidence for hydrogen bonding between β-phosphoryl oxygens of these substrates and the amide nitrogen of glycine in the peptide backbone has been reported (Redfield & Papastavros, 1990; Parmeggianni et al., 1987). *E. coli* glutamine synthetase does *not* contain such a consensus sequence, but the sequence around Lys-47, which is covalently labeled by the ATP analogue 5′-[*p*-(fluorosulfonyl)benzoyl]adenosine and provides the beginning segment of the Trp-57 loop, is Gly-Lys-Met-Phe-Asp-Gly. It is possible that some degeneracy in the consensus sequence may be tolerated and that the Trp-57 loop represents a member of this structural motif of nucleotide binding domains. It may also be noteworthy that a similar sequence is found centered around Trp-57 itself: Gly-Ser-Ser-Ile-Gly-Gly-Trp-Lys-Gly. Here the only residue which interupts one of the consensus sequences found in several nucleotide binding loops is in fact Trp-57. The generality of these sequences in other nucleotide binding proteins, and whether there is a functional analogy between the Trp-57 loop

and other flexible loops which interact with nucleotides, remains to be determined.

The results presented here are consistent with a proposed model in which the relative dynamic natures of Trp-57 and Trp-158 are differentially affected by the addition of the substrate ATP. The Trp-57 loop appears to become less heterogeneous, such that nearly all (90%) of the fluorescence emission is associated with the 5-ns component. Since Trp-158 is much less affected by ATP, it is reasonable to speculate that, under these conditions, ATP binding results in a localized "tightening" of the Trp-57 loop, favoring a conformation which places Trp-57 nearer to the active site and makes it less solvent-accessible (supported by the quenching studies) than the other conformations populated in the absence of ATP. Similar studies with other ligands and under different conditions will provide a detailed description of the conformational states of the protein.

ACKNOWLEDGMENTS

We express our appreciation to Dr. Cathy Royer for enormously helpful suggestions and discussion, and for help in performing the time-resolved fluorescence measurements that were made at the Laboratory for Fluorescence Dynamics at the University of Illinois at Urbana—Champaign (UIUC). We are also grateful to Dr. Joseph Beecham for helpful discussions concerning global analysis. We also gratefully acknowledge Patrice Dombrosky for construction of the W158S mutant.

Registry No. Glu, 56-86-0; ATP, 56-65-5; Trp, 73-22-3; GS, 9023-70-5.

REFERENCES

Alcala, J. R., Gratton, E., & Prendergast, F. G. (1987) *Biophys. J. 51*, 925–936.

Almassy, R. J., Janson, L. A., Hamlin, R., Xuong, N.-H., & Eisenberg, D. (1986) *Nature 323*, 304–309.

Backman, K., Chen, Y.-M., & Magasanik, B. (1981) *Proc. Natl. Acad. Sci. U.S.A. 78*, 3743–3747.

Beechem, J. R., & Gratton, E. (1988) *Proc. SPIE–Int. Soc. Opt. Eng. 909*, 70.

Beechem, J. M., Knutson, J. R., Ross, J. B., Turner, B. W., & Brand, L. (1983) *Biochemistry 22*, 6054–6058.

Cockle, S. A., & Szabo, A. G. (1981) *Photochem. Photobiol. 34*, 22–27.

Colanduoni, J., Nissan, R., & Villafranca, J. J. (1987) *J. Biol. Chem. 262*, 3037–3043.

Colombo, G., & Villafranca, J. J. (1986) *J. Biol. Chem. 264*, 10587–10591.

Dantry-Varsat, A., Cohen, G. N., & Stadtman, E. R. (1979) *J. Biol. Chem. 254*, 3124–3128.

DeBrunner, P. G., & Fraunfelder, H. (1982) *Annu. Rev. Phys. Chem. 33*, 283–299.

Demchenko, A. P. (1986) *Essays Biochem. 22*, 120–156.

Eftnik, M. R., & Wasylewski, Z. (1989) *Biochemistry 28*, 382–391.

Frey, T. G., Eisenberg, D., & Eiserling, F. P. (1975) *Proc. Natl. Acad. Sci. U.S.A. 72*, 3402–3405.

Ginsburg, A. (1972) *Adv. Protein Chem. 26*, 1–59.

Ginsburg, A. Yeh, J., Hennig, S. B., & Denton, M. D. (1970) *Biochemistry 9*, 633–649.

Hennig, B. S., & Ginsburg, A. (1971) *Arch. Biochem. Biophys. 144*, 611.

Hutnik, C. M., & Szabo, A. G. (1989a) *Biochemistry 28*, 3923–3934.

Hutnik, C. M., & Szabo, A. G. (1989b) *Biochemistry 28*, 3935–3939.

Kingdon, H. S., Hubbard, J. S., & Stadtman, E. R. (1968) *Biochemistry 7*, 2136–2142.

Knutson, J. R., Beechem, J. R., & Brand, L. (1983) *Chem. Phys. Lett. 102*, 501–507.

Kunkel, T. A. (1985) *Proc. Natl. Acad. Sci. U.S.A. 82*, 488–492.

Lakowicz, J. R. (1983) *Principles of Fluorescence Spectroscopy*, Plenum Press, New York.

Lakowicz, J. R., & Weber, G. (1973) *Biochemistry 12*, 4161–4170.

Lehrer, S. S. (1971) *Biochemistry 10*, 3254–3260.

McNemar, L. S., Lin, W.-Y., Eads, C. D., Atkins, W. M., Dombrosky, P., & Villafranca, J. J. (1991) *Biochemistry* (second of four papers in this issue).

Meek, T. D., & Villafranca, J. J. (1980) *Biochemistry 19*, 5513–5519.

Meek, T. D., Johnson, K. A., & Villafranca, J. J. (1982) *Biochemistry 21*, 2158–2167.

Miller, R. E., Shelton, E., & Stadtman, E. R. (1974) *Arch. Biochem. Biophys. 163*, 155.

Moss, J., Stanley, S. J., & Levine, R. L. (1988) *FASEB J. 2*, A1045.

Philips, A. U., Coleman, M. S., Masko, S. K., & Barkley, M. D. (1989) *Biochemistry 28*, 2040–2050.

Pinkofsky, H. B., Ginsburg, A., Reardon, I., & Heinrikson, R. L. (1984) *J. Biol. Chem. 259*, 9619–9622.

Pompliano, D. L., Peyman, A., & Knowles, J. R. (1990) *Biochemistry 29*, 3186–3194.

Redfield, A. G., & Papastavros, M. Z. (1990) *Biochemistry 29*, 3509–3514.

Reiman, E. M., Walsh, D. A., & Krebs, E. G. (1971) *J. Biol. Chem. 246*, 1986–1995.

Royer, C., Gardner, J., Beecham, J. M., Brochon, J. C., & Mathews, K. S. (1990) *Biophys. J. 58*, 363–378.

Shapiro, B. M., Kingdon, H. S., & Stadtman, E. R. (1967) *Proc. Natl. Acad. Sci. U.S.A. 58*, 642–649.

Stadtman, E. R., & Ginsburg, A. (1974) *Enzymes (3rd Ed.) 10*, 755–807.

Szabo, A. G., Stepanik, T. M., Wayner, D. M., & Young, N. M. (1983) *Biophys. J. 411*, 233.

Timmons, R. B., Rhee, S. G., Luterman, D. L., & Chock, P. B. (1974) *Biochemistry 13*, 4479–4485.

Valentine, R. C., Shapiro, B. M., & Stadtman, E. R. (1968) *Biochemistry 7*, 2143.

Wierenga, R. K., Terpstra, P., & Hol, W. G. J. (1986) *J. Mol. Biol. 187*, 101–107.

Woolfolk, C. A., Shapiro, B. M., & Stadtman, E. R. (1966) *Arch. Biochem. Biophys. 116*, 177–192.

Yamashita, M. M., Almassy, R. J., Janson, C. A., Lasek, D., & Eisenberg, D. (1989) *J. Biol. Chem. 264*, 17681–17688.